



Reclaimed asphalt binder aging and its implications in the management of RAP stockpiles



Rodolfo Rascon De Lira^{a,*}, Douglas D. Cortes^a, Cesar Pasten^b

^a Civil Engineering Department, New Mexico State University, Las Cruces, NM, USA

^b Civil Engineering Department, University of Chile, Santiago, Chile

HIGHLIGHTS

- The binder content in recycled asphalt pavements (RAP) is particle-size dependent.
- RAP binder aging is particle-size dependent. Small particles age faster.
- Binder from larger RAP particles is expected to experience less extent of oxidation.
- Harvesting and stockpiling larger particles should maximize RAP-binder shelf life.

ARTICLE INFO

Article history:

Received 8 May 2015

Received in revised form 26 September 2015

Accepted 18 October 2015

Keywords:

Reclaimed asphalt pavement
Recycling
Thermoactive composite geomaterial
Geomaterials testing
Asphalt binder aging

ABSTRACT

Reclaimed asphalt pavement (RAP) is a granular composite geomaterial that is highly reactive to the environment under normal atmospheric conditions. The binder aging processes that contribute to pavement deterioration do not stop upon reclamation. Here we report on the results of conventional and a novel RAP characterization test. RAP binder content has been observed to increase as RAP-particle size decreases. A simple analytical model is proposed to explain the results. Binder properties also change as a function of RAP-particle size. A simple thermomechanical test developed as part of this study shows differences in the temperature-dependent deformation of RAP particles of different sizes. These results evidence qualitative differences in binder viscosity, which can be attributed to RAP-binder aging.

© 2015 Elsevier Ltd. All rights reserved.

1. Introduction

Asphalt pavements are major infrastructure assets in the United States and around the world. Billions of dollars are spent annually in resurfacing and reconstruction of asphalt pavements. The reuse of reclaimed asphalt pavements (RAP) in new hot and warm-mix asphalt layers can offer a sustainable alternative for pavement resurfacing and replacement. For this purpose, significant resources and effort have been dedicated to the development of new asphalt pavement mixtures that incorporate high RAP content [1–5]. While sophisticated material characterization methods and mixture design procedures are expected to emerge as a result, basic studies on RAP behavior post reclamation and prior to reuse have not shared the spotlight.

Reclaimed asphalt pavement is a granular composite geomaterial that is highly reactive to the environment under normal atmospheric conditions. The binder aging processes that contribute to the pavement deterioration do not stop upon reclamation. Binder aging is primarily a surface facilitated phenomenon; thus, the reclamation process is expected to accelerate RAP-binder aging by increasing the binder surface exposed to the atmosphere. Furthermore, since the specific surface area of a granular material is particle-size dependent, it is also expected that binder aging will depend on RAP-particle size. The objective of this paper is to explore these hypothetical differences in aging as a function of RAP-particle size. The paper presents a review of binder aging mechanisms in the context of RAP stockpile management followed by the results of a laboratory study designed to explore differences in aging as a function of particle size.

1.1. RAP management practices

Harvesting is the starting point of RAP management. There are two primary harvesting methods: cold milling and ripping and

* Corresponding author at: 3035 S. Espina St., Hernandez Hall Room 202, Las Cruces, NM 88003, USA.

E-mail address: rodo@nmsu.edu (R.R. De Lira).

crushing [2]. Cold milling is the process whereby RAP is harvested using a milling machine down to a desired depth. Ripping and crushing involves the use of heavy machinery that breaks the pavement into small slabs or blocks. The two methods yield RAP with distinct particle sizes. Milling results in smaller particles and high fines content while ripping and crushing produces large particles and low fines content [2,6].

After harvesting, RAP is transported to temporary storage in stockpiles. Available RAP management guidelines [2,6–10] recommend that: (a) RAP should be separated into multiple stockpiles according to source; (b) stockpiles should be constructed in layers to minimize segregation; (c) stockpiles should lay on a base that offers good drainage; (d) stockpiles should be placed over paved surfaces to avoid mixing contamination with soils; and (e) stockpiles should be covered with a roof to minimize moisture infiltration.

Material testing for RAP is limited to the determination of binder content by loss of ignition once every 500–2000 tons of material [11]. While current management practices recognize the importance of maintaining homogenous stockpiles, and of protecting them from further deterioration due to moisture or contaminants, they fail to consider the effects of on-going binder aging during storage.

1.2. Asphalt aging

Asphalt binder is a thermoplastic mixture of various high molecular weight organic compounds. Its chemical composition consists primarily of carbon and hydrogen with minor concentrations of sulfur, oxygen and nitrogen, and trace amounts of vanadium, nickel, and manganese [12]. The organic constituents can be divided into two distinct groups, *asphaltenes* and *maltenes*. Maltenes can in turn be subdivided into saturates, aromatics, and resins. Each of the groups can be subdivided into numerous molecule types; however, the binder rheological properties can be generally traced to the fractions of saturates, aromatics, resins, and asphaltenes, or SARA-fractions [13,14]. Saturates make up between 5% and 20% of the asphalt binder and consist of aliphatic hydrocarbons, alkyl-naphthenes, and some alkyl-aromatics. The saturate molecules are non-polar, and have an average molecular weight in the range of 300–2000 g/mol [14]. The aromatic group constitutes 40–50% of the asphalt binder and comprises the lowest molecular weight naphthenic aromatic compounds (300–2000 g/mol). Molecules are dominated by non-polar carbon chains with unsaturated ring systems. Aromatics readily dissolve other high molecular weight hydrocarbons [14]. The resins group constitute 10–25% of the asphalt binder [15]. Composed primarily of hydrogen and carbon, resins also contain small amounts of oxygen, nitrogen, and sulfur. With molecular weights between 50 and 50,000 g/mol, the typical molecular structure of resins exhibits a polar functional group, an aromatic core, and an aliphatic chain [16]. The polar side of the structure causes resins to interact with electrically charged or polar molecules, while the aliphatic end (being non-polar) yields weak electrical interactions. The unique structure of resins, which causes peptizing of asphaltenes, plays a major role in binder properties [14,17]. Asphaltenes constitute 5–25% of the asphalt binder and comprise highly polar, complex aromatic molecules with very high molecular weights (1000–100,000 g/mol). While all of the maltene components dissolve in *n*-heptane, asphaltenes are insoluble. The asphaltene content and the ratio of asphaltenes-to-resins govern the rheology of asphalt binders [17].

Aging is a complex process that derives from permanent compositional changes in the asphalt binder as a result of its interaction with the atmosphere under prevailing environmental conditions. Hence, both constructed pavement properties and local geospatial conditions determine the evolution of binder aging with

time. Asphalt binder aging causes an increase in the stiffness and brittleness of flexible pavements [18–21]; thus, magnifying its susceptibility to cracking failure and ultimately resulting in a reduction in service life. Binder aging results from four distinct mechanisms: (1) oxidation, (2) volatilization, (3) steric hardening, and (4) exudative hardening.

Oxidation has been recognized as the primary aging mechanism both during construction and in service [13–15,22]. Upon exposure to the atmosphere, oxygen is progressively incorporated into the molecular structure of binder components. This is linked to an increase in polar functional groups that drive the association of molecules into micelles of higher molecular weight [14]. As a result, the binder viscosity increases [23–26].

1.3. Reclaimed asphalt aging

The extent and rate of oxidation of asphalt binder in RAP is controlled by the amount of binder surface exposed to the atmosphere and the exposure time. Hence, oxidation is expected to be inversely related to particle size. Small particles exhibit high specific surface area which increases binder exposure to atmospheric oxygen. In this manuscript, we explore the hypothetical differences in post-harvesting RAP-binder aging as a function of RAP-particle size.

2. Experimental study

RAP harvested using the milling method was collected from stockpiles produced by a local pavement reconstruction project in Southern New Mexico, 6 months after harvesting. The stockpile sampled was uniform and homogeneous and did not show signs of contamination by soil or debris. RAP was brought into the laboratory where the material was sieved and separated into three different particle size fractions: small ($d < 0.425$ mm), medium (0.425 mm $< d < 2$ mm) and large (2 mm $< d < 4.75$ mm). Fig. 1 shows the gradation charts of the original RAP and the separated fractions. Three tests were conducted on each of the RAP-size fractions: (1) binder content, (2) thermomechanical characterization, and (3) Scanning Electron Microscopy (SEM). All testing was carried out within 15–16 months after harvesting.

2.1. Binder content testing

Binder content was determined by exposing the material to a temperature of 580 °C inside a vented furnace. The high temperature causes the organic compounds, i.e., binder, to ignite. Thus, the RAP-binder content can be obtained by determining the mass lost after ignition.

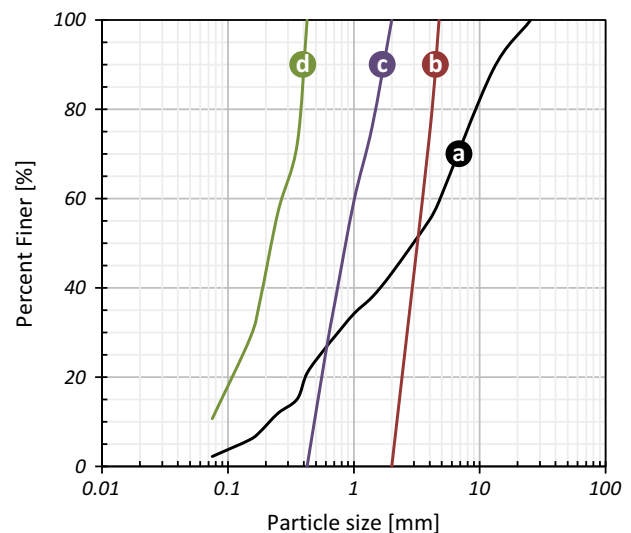


Fig. 1. Grain-size distributions of the RAP specimens tested: (a) original gradation, (b) large size fraction, (c) medium size fraction, and (d) small size fraction.

2.2. Thermomechanical testing

A new test was developed to assess differences in the thermomechanical response of the three RAP-size fractions. A custom-made setup was designed and manufactured to carry out the test (see Fig. 2). Hollow cylindrical molds, 5.08 cm internal diameter and 10.16 cm height, were manufactured with grade 316 stainless steel to resist high temperatures. The test assembly included a reaction frame and a spring which were used to apply vertical stress on the test specimens.

Specimens were prepared by pouring the material inside a mold in three lifts while tamping each lift 25 times. A grade 316 stainless steel cap placed over the final layer served as the base for the spring. The reaction frame was then lowered and fixed in place using hexagonal nut fasteners. The initial spring compression was set at 770 kPa. Three specimens were tested at a time, including two specimens of the same RAP size fraction for repetition, and a specimen of Ottawa sand for control. After 4 h under constant-stiffness load, the vertical deformation for each specimen at room temperature was recorded. The loaded specimens were then placed inside an oven at 30 °C for 4 h. After that, they were removed from the oven and allowed to cool down to room temperature. Further volumetric deformation was then recorded, and the procedure repeated at temperature increments of 20 °C to a maximum temperature of 190 °C.

The temperature dependent viscoelastoplastic deformation is related to the heat-induced softening in the RAP-binder, which in turn is governed by the binder's characteristic viscosity–temperature relationship. All other things being equal, differences in binder properties would result in differences in the temperature-dependent deformation of RAP.

2.3. SEM testing

SEM analysis was conducted using heat-treated mixtures of glass beads and RAP at two particle sizes: large ($2 \text{ mm} < d < 4.75 \text{ mm}$) and small ($d < 0.075 \text{ mm}$). Glass beads were mixed in at a ratio of one third of the total mixture mass. Heat treatment consisted of placing the mixture inside a cylindrical mold, applying a 320 kPa vertical stress, and placing the loaded specimen inside an oven at 170 °C for 4 h. Two specimens were tested at a time, each containing a different RAP size fraction. During heat treatment, the binder is expected to soften and mobilize, effectively coating the surface of glass beads. The specimens were removed from the oven, allowed to cool down, and split in half. Material from within each specimen was collected and processed for the scanning electron microscope (Hitachi S-3400NII).

3. Results and discussion

3.1. Binder content test results

The measured binder contents for each of the RAP size fractions were: $5.8 \pm 0.2\%$ for the small size fraction, $5.6 \pm 0.2\%$ for the medium size fraction, and $4.3 \pm 0.3\%$ for the large size fraction.

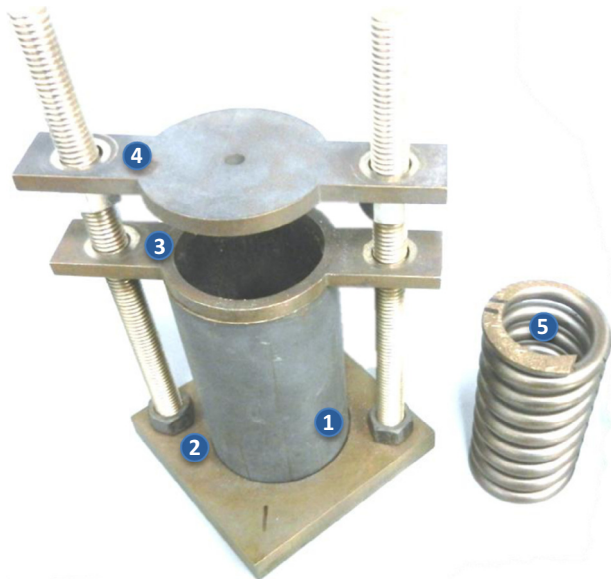


Fig. 2. Custom made thermomechanical test setup: (1) cylindrical mold, (2) base mold support, (3) top mold support, (4) spring reaction frame, and (5) loading spring.

Overall, the binder content in the small and medium size RAP fractions is very similar with only a 3% difference. The binder content in the large size RAP fraction is significantly lower (25% below the other RAP size fractions). The observed differences in binder content from a single source RAP stockpile can be explained by two mechanisms: (1) aggregate particle crushing and (2) binder crushing.

Aggregate particle crushing is governed by stress concentration and the presence of internal flaws within the material. Since flaws occur randomly, crushed particles exhibit irregular shapes [27]. Fig. 3 depicts a RAP particle modeled as a disk aggregate core coated along its periphery by hardened asphalt binder. Note that for the RAP-binder content to be maintained constant across various particle sizes, breakage must yield a sector shape (Fig. 3a). Considering the random distribution of internal flaws, the occurrence of sector shaped breakage would be rather rare. Let's assume instead that breakage occurs in a secant plane such as the one shown in Fig. 3b. The binder content in the two resulting particles after breakage is a function of the breakage angle θ , measured from the disk center to the intersections of the secant breakage plane.

Let r be the radius of the mineral particle and R the extended radius of the bitumen covered particle. The volumetric binder contents of the resulting segments are given by:

$$B'_s = \frac{R^2}{r^2} \left(\frac{\alpha - \sin \alpha}{\theta - \sin \theta} \right) - 1 \quad (1)$$

$$B'_l = \frac{\pi(R^2 - r^2) - 1/2[R^2(\alpha - \sin \alpha) - r^2(\theta - \sin \theta)]}{\pi r^2 - 1/2r^2(\theta - \sin \theta)} \quad (2)$$

where B'_s is the volumetric binder content of the small secant segment and B'_l is the volumetric binder content of the large secant segment, see Fig. 3b. The extended radius of the coated particle R and the angle α are given by:

$$R(r, B) = r\sqrt{B + 1}$$

$$\alpha(r, R, \theta) = 2 \arccos \left[\frac{r}{R} \cos \left(\frac{\theta}{2} \right) \right]$$

where B is the volumetric binder content of the RAP particle prior to breakage. Fig. 3c shows the graphical solution of Eqs. (1) and (2) as a function of θ assuming an initial volumetric binder content of 11.2%; this is an approximate gravimetric binder content of 5.6%. After breakage, the binder content in the large particle segment decreases slightly while the binder content in the smaller particle segment increases substantially, reaching a maximum value of 100% when the breakage plane becomes tangent to the mineral core. Thus, secant-type particle breakage results in an increase in binder content in smaller size RAP fractions.

3.2. Thermomechanical test results

The results of the thermomechanical test performed on the three RAP size fractions are presented in Fig. 4. Volumetric strains in the control (i.e., sand) specimens were null in all cases. Thus, the observed volume changes were caused by the presence of asphalt binder and not by expansion and contraction in the test assembly. Temperature deformation curves in specimens of the same RAP-size fractions were consistent, indicating acceptable repeatability.

The temperature-dependent deformation response can be better compared by normalizing the volumetric strain at each temperature increment by the total volumetric strain in the entire test (Fig. 5).

$$\varepsilon_{vi-norm} = \frac{\varepsilon_{zi}}{\sum_{i=0}^n \varepsilon_{zi}} \quad (3)$$

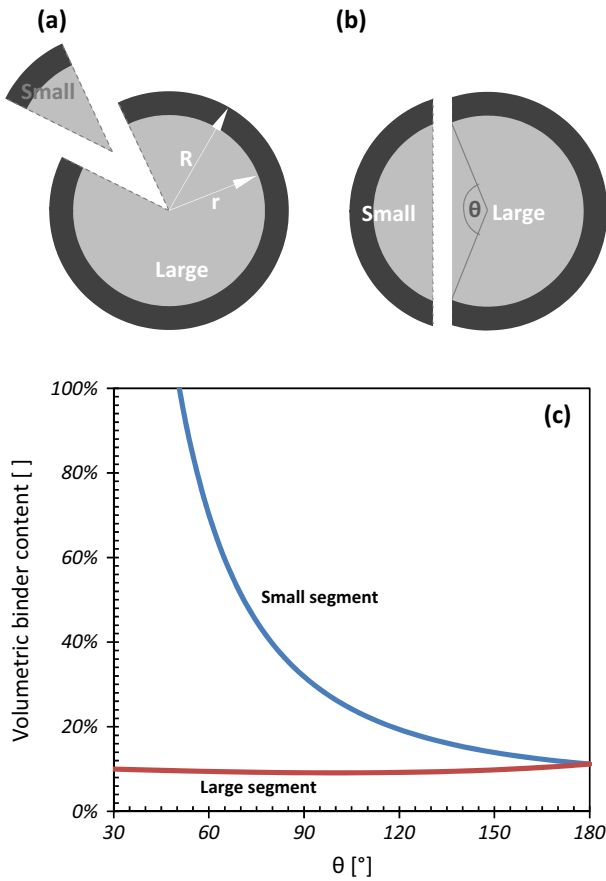


Fig. 3. Geometric analysis of particle breakage in disk shaped RAP particles. (a) Binder content is only preserved when breakage occurs in sectors. (b) Secant breakage planes (dashed line) result in an increase in binder content on small particles. (c) The small-particle segment binder content is a function of the breakage angle, θ , for secant breakage planes.

where ε_{zi} is the axial strain at i th temperature increment. Note that under zero lateral strain loading the volumetric strain is equal to the axial strain.

In large-size RAP particles (Fig. 5a), a third of the total volumetric strain is attained at temperatures below 36 °C. Two thirds of the total volumetric strain are attained at temperatures below 55 °C, and the total volumetric strain is attained at temperatures below 120 °C.

In medium-size RAP particles (Fig. 5b), a third of the total volumetric strain is attained at temperatures below 43 °C. Two thirds of the total volumetric strain are attained at temperatures below 62 °C, and the total volumetric strain is attained at temperatures below 120 °C.

In small-size RAP particles (Fig. 5c), a third of the total volumetric strain is attained at temperatures below 48 °C. Two thirds of the total volumetric strain are attained at temperatures below 66 °C, and the total volumetric strain is attained at temperatures below 120 °C.

Comparatively, a decrease in RAP-particle size causes a shift in the deformation curve toward higher temperature. Since the temperature deformation curve is inherently controlled by the binder's characteristic viscosity-temperature relationship, differences in the temperature-dependent viscoelastoplastic deformation across RAP-size fractions indicate differences in binder properties. A shift in the temperature-deformation curve toward higher temperature is indicative of higher viscosity RAP-binder, i.e., higher temperature is required to soften the binder and drive the volumetric deformation. Thus, the experimental results support the hypothe-

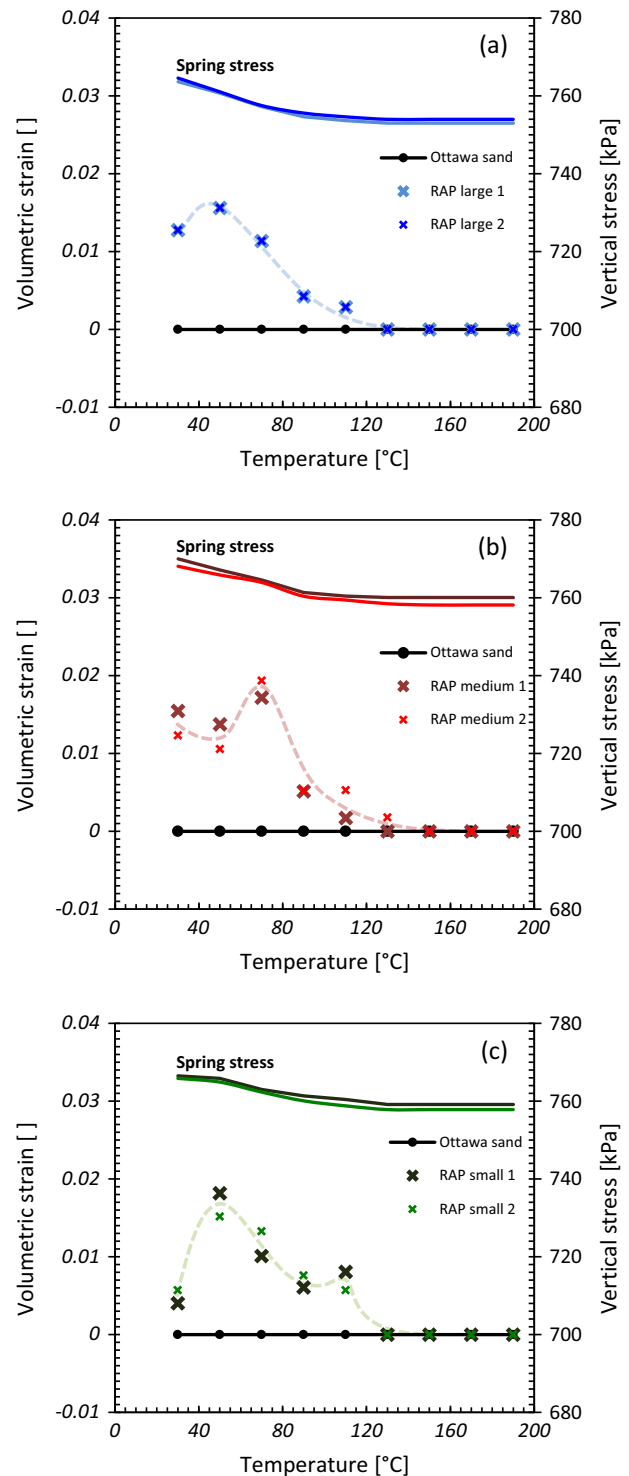


Fig. 4. Mobilized volumetric strain as a function of temperature for (a) large, (b) medium, and (c) small particle RAP specimens. Lines at the top of each graph show the change in stress applied by the spring throughout the test. The net stress reduction never exceeded 2.5%.

sis that a reduction in RAP-particle size leads to an increase in RAP-binder aging.

3.3. Complementary SEM study

Captured SEM images of the glass-RAP mixtures reveal qualitative differences in the asphalt binder between large and small RAP

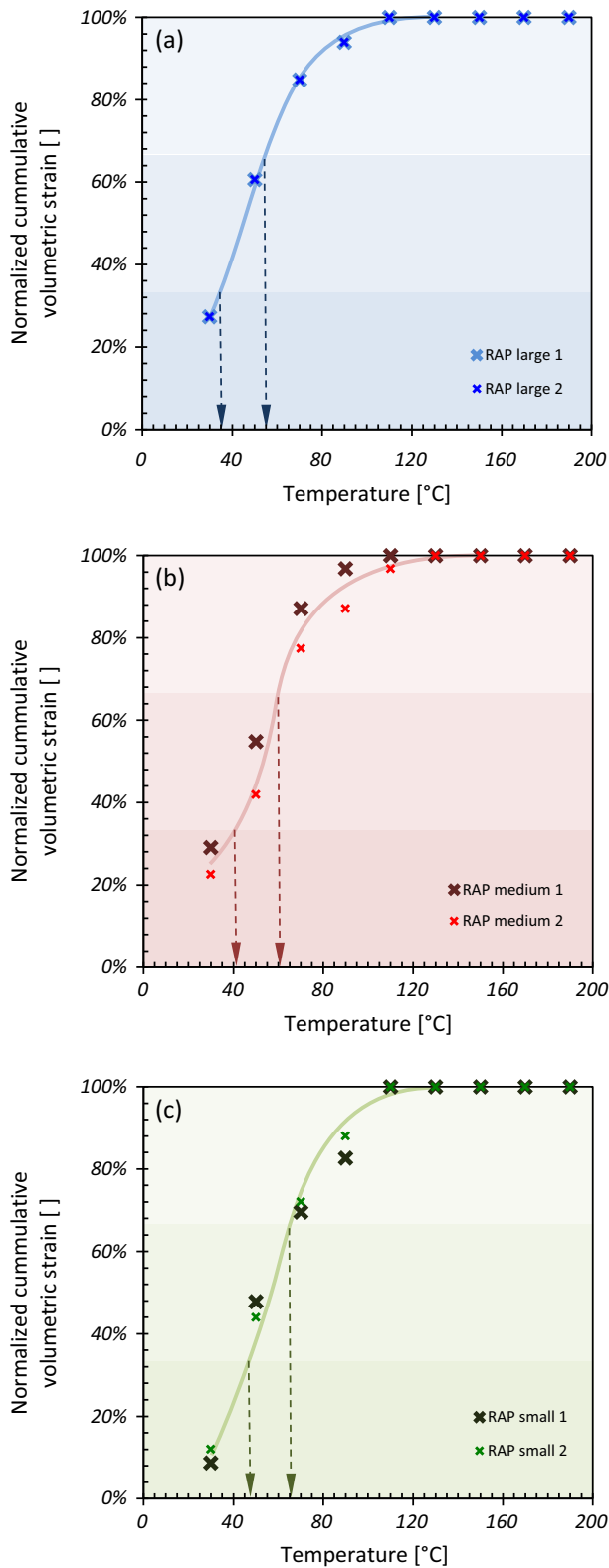


Fig. 5. Normalized volumetric strain–temperature evolution for (a) large, (b) medium, and (c) small particle size RAP specimens.

particles. In the case of large RAP particles (Fig. 6), the binder mobilizes and coats glass particles upon heating. As the temperature decreases the binder solidifies rendering a solid bond between glass and RAP. The presence of menisci and the extent of coating are

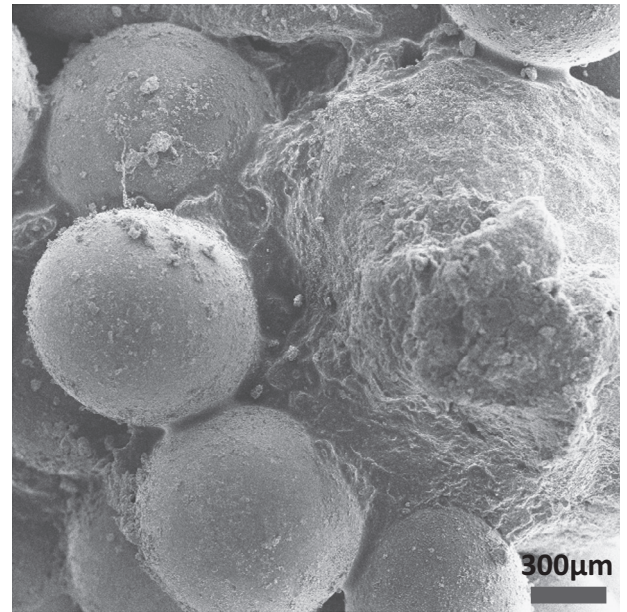


Fig. 6. Heat treated mixture of large RAP particles and glass beads. Binder softens upon heating and mobilizes coating glass bead particles and forming menisci. Upon cooling the binder solidifies rendering glass bead particles bonded.

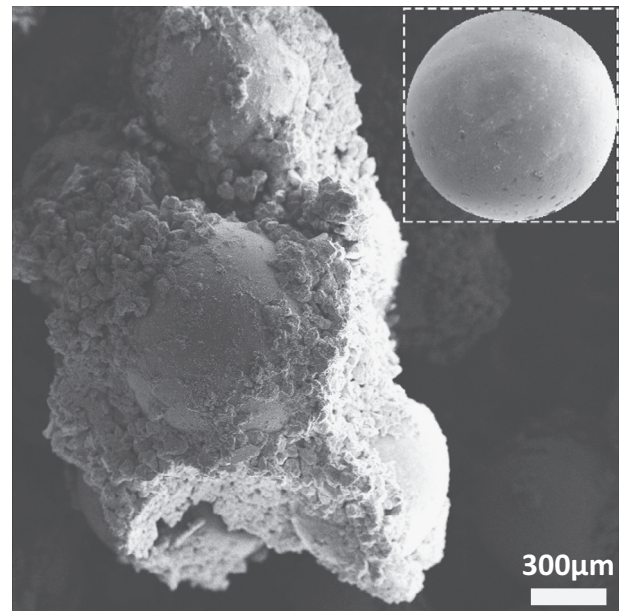


Fig. 7. Heat treated mixture of small RAP particles and glass beads. Salient features are clusters of small particles attached to each other and to the glass particles. Crater-like structures remain after detachment, where glass beads used to be.

consistent with lower viscosity binder. In the case of small RAP particles (Fig. 7), the SEM images reveal a significantly different interaction between the glass beads and RAP. Unlike the coatings and menisci observed in large RAP particles, the salient features are clusters of small particles attached to each other and to the glass particles. Crater-like features remain after detachment, where glass beads used to be. The morphology could be described as ‘sintered’ RAP particles that have undergone viscoplastic deformation at the glass–RAP interface. The results of the test with small RAP particles appear consistent with a higher viscosity asphalt binder.

4. Conclusions

A combination of novel thermomechanical tests and high resolution microscopy has been used to characterize the behavior of reclaimed asphalt pavement as a function of particle size. It has been found that:

- (1) The binder content in RAP is particle-size dependent. As a result of crushing, smaller RAP particles exhibit higher binder content.
- (2) The degree of aging of the binder is also particle-size dependent. For the same duration of exposure to atmospheric oxygen, the binder in smaller RAP particles attains a higher degree of aging.

4.1. Implications in the management of reclaimed asphalt stockpiles

Crushing of asphalt pavement into RAP causes an increase in binder oxidation rate. Thus, in stockpiles RAP-binder has a shelf life.

At any given time, the properties of binder recovered from a RAP stockpile are particle-size dependent. Binder from larger RAP particles is expected to experience a lesser extent of oxidation. Thus, harvesting and stockpiling larger particles should maximize RAP-binder shelf life.

RAP-binder content is particle size dependent. Smaller particles exhibit higher binder content; however, binder in smaller RAP particles is more susceptible to oxidation. Thus, high binder contents do not necessarily imply high potential for binder replacement in new asphalt mixtures.

Acknowledgements

Support for this research was provided by the New Mexico Department of Transportation, the US Federal Highway Administration, start-up funding from the College of Engineering and the Civil Engineering Department at New Mexico State University, and the joint Ph.D. program between New Mexico State University and Universidad Autónoma de Chihuahua.

References

- [1] A. Copeland, J. D'Angelo, R. Dongre, S. Belagutti, G. Sholar, Field evaluation of high reclaimed asphalt pavement-warm-mix asphalt project in Florida, *Transport. Res. Rec.: J. Transport. Res. Board* 2179 (2010) 93–101.
- [2] P.S. Kandhal, R.B. Mallick, *Pavement Recycling Guidelines for State and Local Governments Participant's Reference Book*, 1998.
- [3] D.E. Newcomb, E.R. Brown, J.A. Epps, A. National Asphalt Pavement, *Designing HMA Mixtures with High RAP Content: A Practical Guide*, National Asphalt Pavement Association, 2007.
- [4] R.C. West, J.R. Willis, M.O. Marasteanu, Improved mix design, evaluation, and materials management practices for hot mix asphalt with high reclaimed asphalt pavement content, *Transport. Res. Board*, 2013.
- [5] S. Zhao, B. Huang, X. Shu, X. Jia, M. Woods, Laboratory performance evaluation of warm-mix asphalt containing high percentages of reclaimed asphalt pavement, *Transport. Res. Rec.: J. Transport. Res. Board* 2294 (2012) 98–105.
- [6] P. Lavin, *Asphalt Pavements: A Practical Guide to Design, Production and Maintenance for Engineers and Architects*, CRC Press, 2003.
- [7] W.H. Chesner, R.J. Collins, M.H. MacKay, *User Guidelines for Waste and By-product Materials in Pavement Construction*, 1998.
- [8] A. Copeland, *Reclaimed Asphalt Pavement in Asphalt Mixtures: State of the Practice*, 2011.
- [9] K. Nassar, W. Nassar, Reclaimed asphalt pavement detection and quantity determination, *Pract. Period. Struct. Des. Constr.* 11 (2006) 171–176.
- [10] F. Zhou, G. Das, T. Scullion, S. Hu, *Rap Stockpile Management and Processing in Texas: State of the Practice and Proposed Guidelines*, 2010.
- [11] R. West, Summary of NCAT Survey on RAP Management Practices and RAP Variability, vol. 6, Federal Highway Administration, Washington, DC. <<http://www.morerap.us/RAP%20Resources/reports.html>>, site last accessed January, 2008, p. 2011.
- [12] W.D. Fernández-Gómez, H. Rondón Quintana, F. Reyes Lizcano, A review of asphalt and asphalt mixture aging, *Rev. de Ing. e Inv.* 33 (2013).
- [13] J.C. Petersen, A review of the fundamentals of asphalt oxidation: chemical, physicochemical, physical property, and durability relationships, *Transport. Res. E – Circ.* (2009).
- [14] J. Read, D. Whiteoak, *The Shell Bitumen Handbook*, Thomas Telford, 2003.
- [15] A. Srivastava, R. van Rooijen, Bitumen performance in hot and arid climates, in: *Proc. Innovative Road Rehabilitation and Recycling Technologies; Pavement Seminar for the Middle*, 2000, pp. 24–26.
- [16] A. Hunt, Uncertainties remain in predicting paraffin deposition, *Oil Gas J.* 94 (1996) 96–103.
- [17] J.F. Schabron, J.G. Speight, The solubility and three-dimensional structure of asphaltenes, *Pet. Sci. Technol.* 16 (1998) 361–375.
- [18] WRI, *Asphalt Surface Aging Prediction (ASAP) System*, Western Research Institute No. DTOS59-07-H-0006, 2010.
- [19] M.O. Imbarek, M.K. All, Hardening and aging of bituminous materials in hot arid regions, in: *Performance of Bituminous and Hydraulic Materials in Pavements: Proceedings of the Fourth European Symposium*, Nottingham, UK, 2002, pp. 25–31.
- [20] A. Kumar, W.H. Goetz, Asphalt hardening as affected by film thickness, voids and permeability in asphaltic mixtures, in: *Association of Asphalt Paving Technologists Proc*, San Antonio, TX, 1977, pp. 571–605.
- [21] N.A. Al-Azri, S.H. Jung, K.M. Lunsford, A. Ferry, J.A. Bullin, R.R. Davison, et al., Binder oxidative aging in Texas pavements: hardening rates, hardening susceptibilities, and impact of pavement depth, *Transport. Res. Rec.: J. Transport. Res. Board* 1962 (2006) 12–20.
- [22] J.S. Chen, L.S. Huang, Developing an aging model to evaluate engineering properties of asphalt paving binders, *Mater. Struct.* 33 (2000) 559–565.
- [23] J.F. McKay, P.J. Amend, T.E. Cogswell, P.M. Harnsberger, R.B. Erickson, D.R. Latham, Petroleum asphaltenes: chemistry and composition, *Prepr. Div. Pet. Chem. Am. Chem. Soc. (United States)* 22 (1977).
- [24] H. Reerink, Size and shape of asphaltene particles in relationship to high-temperature viscosity, *Ind. Eng. Chem. Prod. Res. Dev.* 12 (1973) 82–88.
- [25] R.L. Griffin, W.C. Simpson, T.K. Miles, Influence of composition of paving asphalt on viscosity, viscosity-temperature susceptibility, and durability, *J. Chem. Eng. Data* 4 (1959) 349–354.
- [26] W.C. Simpson, R.L. Griffin, T.K. Miles, Relationship of asphalt properties to chemical constitution, *J. Chem. Eng. Data* 6 (1961) 426–429.
- [27] M.S. Guimaraes, J.R. Valdes, A.M. Palomino, J.C. Santamarina, Aggregate production: fines generation during rock crushing, *Int. J. Miner. Process.* 81 (2007) 237–247.